Effects of Pressure Ratio on Population Inversion in a DF Chemical Laser with Concurrent Lasing

Jun Sung Park and Seung Wook Baek
Division of Aerospace Engineering, Department of Mechanical Engineering
Korea Advanced Institute of Science and Technology
373-1 Guseong-dong, Yuseong-gu, Daejeon 305-701, Republic of Korea
jimmy@kaist.ac.kr swbaek@kaist.ac.kr

Keywords: DF chemical laser, D_2 injection pressure, Population inversion

Abstract

A numerical simulation is presented for investigating the effects of pressure ratio of D_2 injector to supersonic nozzle on the population inversion in the DF chemical laser cavity, while a lasing concurrently takes place. The laser beam is generated between the mirrors in the cavity and it is important to obtain stronger population inversion and more uniform distribution of the excited molecules in the laser cavity in order to produce high power laser beam with good quality. In this study, these phenomena are investigated by means of analyzing the distributions of the DF excited molecules and the F atom used as an oxidant, while simultaneously estimating the maximum small signal and saturated gains and power in the DF chemical laser cavity. For the numerical solution, an 11-species (including DF molecules in various excited states of energies), 32-step chemistry model is adopted for the chemical reaction of the DF chemical laser system. The results are discussed by comparison with two D_2 injector pressure cases; 192 torr and 388.64 torr. Major results reveal that in the resonator, stronger population inversions occur in the all transitions except DF(1)-DF(0), when the D_2 injection pressure is lower. But, the higher D_2 injection pressure provides a favorable condition for DF(1)-DF(0) transition to generate the higher power laser beam. In other words, as the pressure of D_2 injector increases, the maximum small signal gain in the v_{1-0} transition, which is in charge of generating most of laser power, becomes higher. Therefore, the total laser beam power becomes higher.

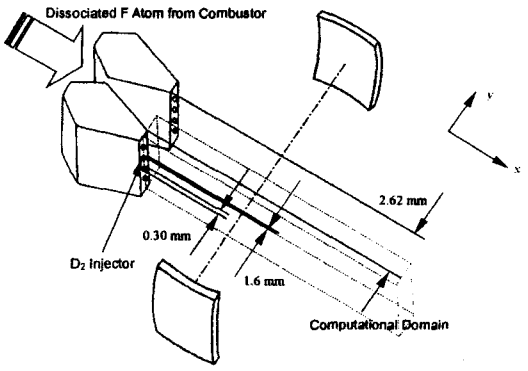

Fig. 1 DF chemical laser cavity

Introduction

A chemical laser can generate high power laser beam in the megawatt range, which may be used for manufacturing processes in industries or military purposes.

Laser operation takes place via transitions between different energy levels of an atomic or molecular system. Therefore there always have to be the excited atoms or molecules in the laser system, which are usually created by use of a light source like diode or lamp. But the chemical laser makes use of the only chemical reaction in order to produce the excited atoms or molecules. It is more advantageous to exploit a considerable amount of chemical energy produced from chemical reactions to generate the excited atoms or molecules, since the chemical laser has a characteristic of considerably high efficiency in energy transformation from chemical energy to light energy.

Although the chemical laser has such an advantage, the expansion process through a supersonic nozzle is particularly necessary to keep the unstable excited atoms or molecules in pretty long time. Very complicated flow patterns comprising strong shock and expansion waves occur. The F atom used as an oxidant is expanded through a supersonic nozzle while forming a low vacuum environment (5~10 torr). Then, in the cavity an intense laser beam is generated through the reaction of F with H_2 or D_2.

There have been several experimental as well as analytical or numerical studies that examined HF and DF chemical lasers. An analytic model characterizing diffusion flames and premixed systems in the chemical laser was made by Emanuel[1]. Especially, a behavior of premixed systems involving the cold reaction and the influence of *j*-shifting on the performance were examined. Skifstad[2] presented a theory for an HF chemical laser employing both the hot and cold pumping reactions under continuous wave conditions. The influence of numerous parameters of the system on the specific power output, gain and saturation was discussed therein.

King and Mirels[3] numerically investigated the performance of an HF diffusion-type chemical laser for the laminar diffusion of a finite stream of H_2 into a semi-infinite stream containing F and a diluent. An analytical treatment of diffusion-type chemical lasers was presented using a single-boundary-layer and flame-sheet model by Hofland and Mirels[4, 5]. The

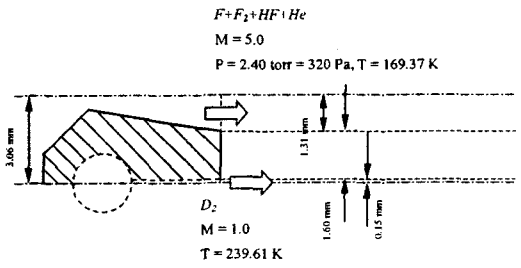

Fig. 2 A schematic of the DF chemical laser cavity

chemical formation of lasing molecules was modeled by diffusion-controlled mixing and combustion of parallel streams of fuel and oxidizer, while the coupled collisional and radiative relaxation of vibrationally excited lasing diatomics were considered for the limiting case of a radiatively saturated medium.

In 1980s, Driscoll[6, 7] performed experiments as well as numerical simulations to demonstrate the ability of a new supersonic ramp nozzle design to accelerate mixing in a DF chemical laser via the reactant surface stretching mechanism. It revealed a possible mechanism by which the reactant surface stretching caused by trip jets could enhance mixing.

The purpose of the present study is to describe the effects of the pressure ratio across D_2 injector in supersonic nozzle on the population inversion as well as lasing power in the DF chemical laser cavity. By varying D_2 injection pressure with a simple geometric cavity block comprising the supersonic nozzle, D_2 injector and nozzle base, the characteristics of mixing and reacting phenomena are to be examined and discussed while considering a laser power generation.

Governing Equations

As schematized in Fig. 1, the current paper deals with supersonic chemical reaction with generation of laser beam in the DF chemical laser cavity. These phenomena are governed and solved by the Navier-Stokes equations, species conservation equations and radiative transport equation with variable thermo-physical properties.

In the upper section of the physical model adopted in this study, a uniform mixture comprising F, F_2, HF and He is supposed to flow into the chemical laser cavity through the supersonic nozzle at M = 5.0, P = 2.40 torr and T = 169.3 K as shown in Fig. 2. In the lower section, the sonic D_2 is injected in parallel at T = 239.61 K. There is a nozzle base between the supersonic nozzle and D_2 injector with a height of 1.6 *mm*, which is considered to play an important role in the mixing process. The DF chemical laser cavity in this study is considered to consist of 10 nozzles array and a resonator with the length of optical axis equal to 61.2 *mm*.

Governing Equations

The governing equations for the above problem are the time-dependent compressible Navier-Stokes equations in a strongly conservative form. The unsteady conservation equations are in the following form:

$$\frac{\partial Q}{\partial t}+\frac{\partial E}{\partial x}+\frac{\partial F}{\partial y}=\frac{\partial E_v}{\partial x}+\frac{\partial F_v}{\partial y}+S_{chem}+S_{rad}, \quad (1)$$

where Q is the conservative flow variable vector, and E and F are the inviscid flux vectors in the x, y directions, respectively. E_v and F_v are the viscous flux vectors. Finally, S_{chem} and S_{rad} are source vectors that represent the rates of formation of chemical species due to the chemical reaction and the stimulated emission, respectively. Each vector is defined in the previous study[8] and source vectors are particularly expressed as below:

$$S_{chem}=\begin{bmatrix}0\\0\\0\\0\\\omega_i\end{bmatrix},\ S_{rad}=\begin{bmatrix}0\\0\\0\\-\sum_{v}\sum_{J}\alpha_{v,J}I_{v,J}\\\omega_{rad,J}\end{bmatrix}.$$

To close the system of equations (1), the equation of state needs to be introduced. The macroscopic thermodynamic properties of the gas are related through the general equation of state.

Chemical Reaction Model

Besides thermo-chemical and fluidic conditions imposed, the chemical reaction model would play an extremely important role in analyzing the DF chemical lasing processes. Because a high speed gas is expanding through a supersonic nozzle into the cavity in a very short time, its phenomena may not be simply described by the single step chemical reaction. Instead the multi-step chemical reaction model has to be applied as follows:

$$\sum_{j=1}^{NS}v_{ij}^{'}n_j \underset{k_{b_i}}{\overset{k_{f_i}}{\rightleftharpoons}} \sum_{j=1}^{NS}v_{ij}^{''}n_j,\ i=1,2,\cdots,N_R, \quad (2)$$

where $v_{ij}^{'}$ and $v_{ij}^{''}$ represent the stoichiometric coefficients of the j th reactants and products for i th chemical reaction step. n_j is the molar concentration of the j th species. NS and N_R are, respectively, the number of chemical species involved in the chemical reactions and the total number of the chemical reaction step. k_{f_i} and k_{b_i} are the forward and backward reaction rate constants, which are experimentally determined and expressed by the Arrhenius type as follows:

$$k_i=A_iT^{m_i}e^{-E_i/R_uT}, \quad (3)$$

where E_i is the activation energy, and A_i and m_i are all determined using experimental data.

For the chemical reaction (2), the rate of change of mass concentration for the j th species becomes

$$\omega_j=W_j\sum_{i=1}^{N_R}\left[\left(v_{ij}^{''}-v_{ij}^{'}\right)\left(k_{fi}\prod_{l=1}^{NS}n_l^{v_{il}^{'}}-k_{bi}\prod_{l=1}^{NS}n_l^{v_{il}^{''}}\right)\right]. \quad (4)$$

In the present study, the 32-step chemistry model for 11-species (including DF molecules in various

excited states), is adopted for the DF reaction occurring in cavity.

Radiative Transfer Equation

A monochromatic, unidirectional light emitted by a laser is electromagnetic radiation. Therefore, in order to analyze the laser beam characteristics and its power, the radiative transport equation is needed to deal with the electromagnetic radiation. The fundamental equation for radiative transfer in the laser cavity can be written by

$$\pm\frac{\partial I^{\pm}_{v,J}}{\partial y}=\alpha_{v,J}I^{\pm}_{v,J}, \quad (5)$$

where $I^{\pm}_{v,J}$ is the intensity of radiation in the spectral line from (v+1, J-1) to (v, J) propagating in the $\pm y$ direction. And $\alpha_{v,J}$ is the optical gain coefficient that is evaluated[9]. Assuming that the plane-parallel mirrors are located at both end sides of y axis, the appropriate boundary conditions are

$$I^{+}_{v,J}=r_0 I^{-}_{v,J} \text{ at } y=0,\ I^{-}_{v,J}=r_{L_{axis}} I^{+}_{v,J} \text{ at } y=L_{axis}, \quad (6)$$

where r_0 and $r_{L_{axis}}$ are the mirror reflectivities of which values used in this system are, respectively, 0.87 and 1.0.

$\omega_{rad,i}$ in the source vector S_{rad} of species equation (1) illustrates the rate of formation of i th chemical species due to the stimulate emission. However, this term is not zero only when the chemical species are DF molecules in the DF chemical laser. Its rate of formation of the excited DF molecule is expressed as follows:

$$\omega_{rad,i}=\frac{W_{DF}}{\hbar N_A}\sum_J\left(\frac{\alpha_{v,J}I_{v,J}}{\nu_{v,J}}-\frac{\alpha^{v,J}I^{v,J}}{\nu^{v,J}}\right). \quad (7)$$

The subscript or superscript v, J represents a P-branch transition from (v+1, J-1) to (v, J) or the one from (v, J) to (v-1, J+1), respectively.

Numerical Method

Equation (1) constitutes the hyperbolic type of equations, of which each variable is closely coupled each other. There exist a lot of numerical methods for solving this type of system. In the present analysis, the finite volume method (FVM) is employed since this method is known to easily satisfy the conservation rules and to be computationally stable at the surface of discontinuities.

First of all, in order to enhance the numerical efficiency and conveniently apply the physical boundary conditions, a physical space is transformed into a computational space. Then, the equation (1) becomes

$$\frac{\partial\overline{Q}}{\partial t}+\frac{\partial\overline{E}}{\partial\xi}+\frac{\partial\overline{F}}{\partial\eta}=\frac{\partial\overline{E}_v}{\partial\xi}+\frac{\partial\overline{F}_v}{\partial\eta}+\overline{S}_{chem}+\overline{S}_{rad}, \quad (8)$$

where

$$\overline{Q}=\frac{1}{J}Q,\ \overline{E}=\frac{1}{J}\left(\xi_x E+\xi_y F\right),\ \overline{F}=\frac{1}{J}\left(\eta_x E+\eta_y F\right),$$

Table 1 DF chemical laser inlet conditions

	F Nozzle		D_2 Injector	
Mach Number	5.0			1.0
Temperature (K)	169.37			239.61
Pressure (torr)	2.40			388.64
				192.00
Species Mass Fraction	F	0.3071	D_2	1.0
	F_2	0.0340		
	HF	0.3191		
	He	0.3398		

$$\overline{E}_v=\frac{1}{J}\left(\xi_x E_v+\xi_y F_v\right),\ \overline{F}_v=\frac{1}{J}\left(\eta_x E_v+\eta_y F_v\right),$$

$$\overline{S}_{chem}=\frac{1}{J}S_{chem},\ \overline{S}_{rad}=\frac{1}{J}S_{rad}.$$

Jacobian, J represents the volume of each cell in the Cartesian coordinate system.

In order to solve the equation (8) in the generalized coordinate, Roe's average[10] and the 2nd order TVD (Total Variation Diminishing) scheme[11, 12] are used together with the finite volume method (FVM), thereby improving the resolution of discontinuities in a reacting compressible flow. For TVD scheme, the limiter employed is a less compressive van Leer limiter for nonlinear fields, while a more compressive superbee limiter for the linear fields. And the entropy correction[11, 12] is used with δ = 0.01 in order to prevent the unphysical solutions from occurring through a correction of the eigenvalues in the flux Jacobian matrix.

Time Stepping Method

To solve the equations with the conservative vector variables, the LU decomposition proposed by Jameson and Turkel[13] is used, since it has the advantage in reducing the computational efforts in calculating the inverse matrices.

In this analysis, although the final solutions are steady state ones, the calculation is numerically unstable at the early stage, which is especially caused by the nozzle base located between the supersonic nozzle and the D_2 injector. Hence, the time interval used here is the smallest one among the allowable time steps for each cell in the unsteady problem.

Boundary Conditions

In this analysis of the DF chemical laser cavity, the boundary conditions have to be imposed on upper and lower walls, inlet and outlet as shown in Fig. 2. The outlet condition is necessary since the flow is recirculating behind supersonic nozzle base.

At upper and lower walls, the symmetric condition is applied since the physical domain is a part of the nozzle array. At the outlet, the outflow condition of the 1st order extrapolation is used, because the flow speed is supersonic. Finally, the boundary conditions at the supersonic nozzle and the D_2 injector are given in Table 1, while the adiabatic conditions are applied at the nozzle base.

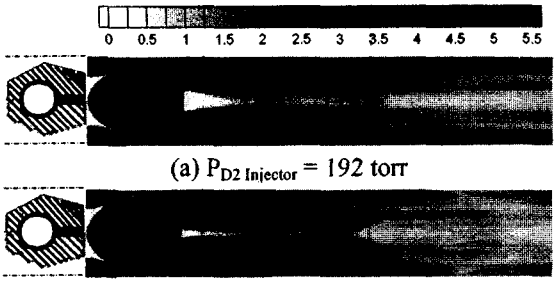

(a) $P_{D2\ Injector}$ = 192 torr

(b) $P_{D2\ Injector}$ = 388.64 torr

Fig. 3 Effects of D_2 injector pressures on the Mach contours

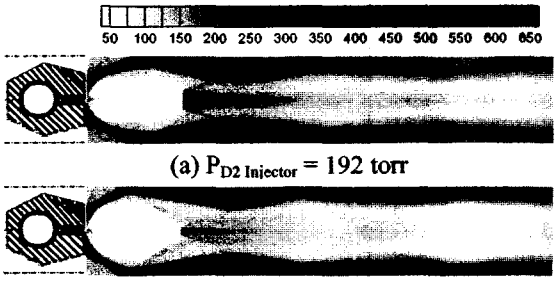

(a) $P_{D2\ Injector}$ = 192 torr

(b) $P_{D2\ Injector}$ = 388.64 torr

Fig. 4 Effects of D_2 injector pressures on the temperature contours

In order to calculate the intensity distributions, the boundary conditions expressed in the equation (6) are applied. The cavity block is supposed to consist of 10 nozzle blocks in the y direction. The resonator is equipped with two flat mirrors of which separate distance is 61.2 *mm*. The width of a mirror is 5 *cm* while one end of the mirror is located at the nozzle exit ($x = 0$ *cm*).

Results and Discussion

Now, the effects of D_2 injection pressure on the population inversion in the laser cavity are to be discussed when lasing occurs concurrently. The pressure ratio is directly connected with the D_2 mass flow rate injected from the D_2 injector. As the pressure ratio increases, the mass flow rate of D_2 from the D_2 injector linearly increases. When the mass fraction and the temperature are kept constant at the inlet as presented in Table 1, this linear proportionality between the pressure ratio and the mass flow rate is preserved according to the equation of state.

In this study, F atom reacts with D_2 molecule to produce the excited molecules, DF(i=0~4), which are supposed to have different energy states. It is necessary to calculate their concentrations to estimate the lasing power as done before by King and Mirels for HF system[3]. Two D_2 injection pressure conditions of 192 and 388.64 torr are examined here, while the other inlet conditions are kept constant. The flow in the laser cavity is believed to be laminar according to

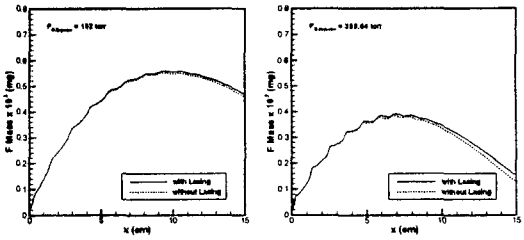

(a) $P_{D2\ Injector}$ = 192 torr (b) $P_{D2\ Injector}$ = 388.64 torr

Fig. 5 Comparison of F atom mass distributions with respect to longitudinal distance x from the nozzle exit plane

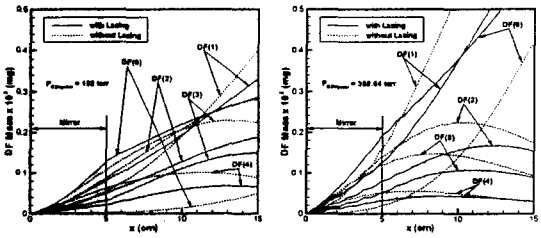

(a) $P_{D2\ Injector}$ = 192 torr (b) $P_{D2\ Injector}$ = 388.64 torr

Fig. 6 Effects of the D_2 injection pressures on the mass distribution of the excited DF molecules with respect to longitudinal distance x from the nozzle exit plane plane

Masuda *et al.*[8], since the Reynolds number based on the size of D_2 injector (0.3 *mm*) and the injection conditions is of the order of 10^2.

Fig. 3 illustrates the effects of D_2 injection pressures on the Mach contours. A strong expansion is observed to occur near the D_2 injector as soon as D_2 is injected, since D_2 injection pressure is much higher than the static pressure of fluorine mixture. And the recirculation zone is generated around the base between the D_2 injector and supersonic nozzle. The peculiar differences between 192 torr and 388.64 torr cases reside in the height of the Mach disc and the inclined angles of shock wave surfaces behind the Mach disc as shown in Fig. 3. As the pressure of the D_2 injector increases, a stronger shock wave is formed while influencing flow field so that a stronger reflected shock wave is also set up. Consequently, the pattern of the shock wave reflection becomes more apparent for higher D_2 injection pressure. A similar discussion applies to the temperature contours plotted in Fig. 4, which reveals that the strength of the reflected shock wave is higher for the higher D_2 injection pressure, although it is getting weaker along the downstream. While for the D_2 injection pressure of 192 torr, the maximum temperature (~700 *K*) is located near the recirculation zone, it (~800 *K*) occurs at the intersection of the upper symmetric line and the first reflected shock wave for 388.64 torr case. Therefore, as the pressure ratio increases, the chemical reaction becomes more active that more DF excited

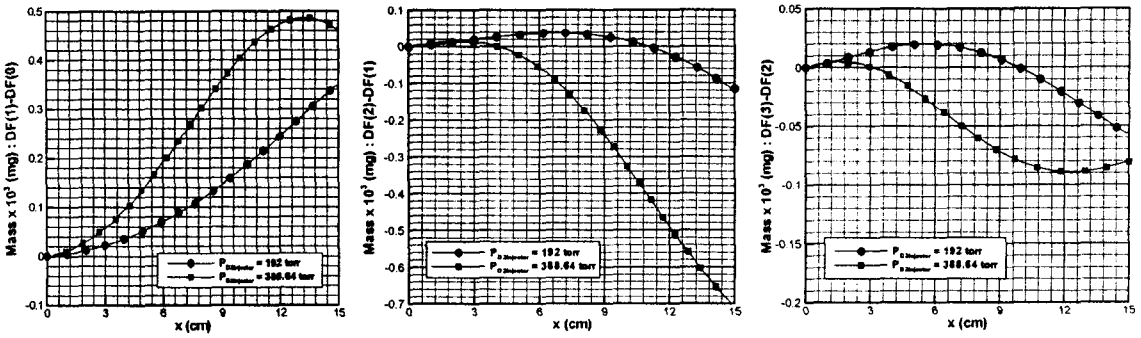

(a) DF(1)-DF(0) (b) DF(2)-DF(1) (c) DF(3)-DF(2)

Fig. 7 Effects of the D_2 injection pressures on the mass distributions of DF(i)-DF(i-1) (i=1~3) with respect to longitudinal distance x from the nozzle exit plane for the cases without lasing

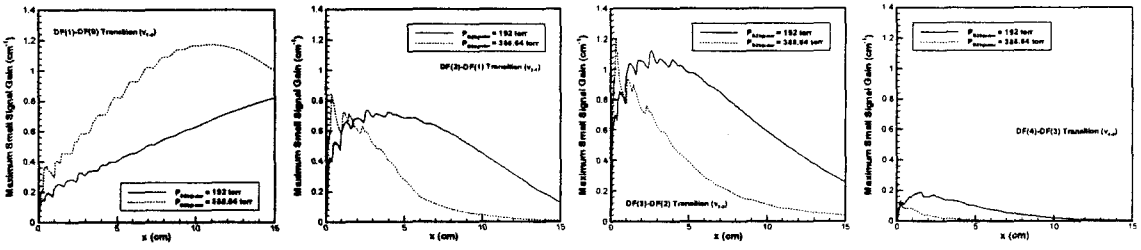

(a) v_{1-0} transition (b) v_{2-1} transition (c) v_{3-2} transition (d) v_{4-3} transition

Fig. 8 Various maximum small signal gain distributions with respect to longitudinal distance x from the nozzle exit plane

molecules might be produced and the population inversion is greater.

As a matter of fact, more F atoms are consumed for the higher D_2 injection pressure as plotted in Fig. 5, since the chemical reaction capable of producing the excited DF molecules becomes more active as mentioned before. When the resonator, which is composed of mirrors and cavity, is set up for lasing, less F atoms are observed to be consumed along the longitudinal distance. The reason is that the temperature becomes a little lower when lasing occurs due to the stimulated emission term in the energy equation (1), $-\sum_{v}\sum_{J}\alpha_{v,J}I_{v,J}$ which is negative.

Fig. 6 shows the mass distributions of the excited DF molecules along the axial distance x from the nozzle exit plane. For the case with lasing, the population inversion is observed in the limited domain (x=0~0.5 *cm*). After this, more excited DF molecules are found in lower energy level within the resonator (0.5~5 *cm*) and farther downstream, since DF molecules in higher energy level degenerate to those in lower energy level due to lasing. However, for the case without lasing, the population inversion phenomena can be seen in wider range, for lasing does not occur. In order to examine it in more detail, Fig. 7 is plotted, which reveals that in the resonator, a stronger population inversion occurs in the all of energy transitions except the one of DF(1)-DF(0) as the D_2 injection pressure is lower. However, the case of 388.64 torr shows a large mass difference between DF(1) and DF(0), which provides a favorable condition to generate the high power laser beam, since most of power in the DF chemical laser is generated in the DF(1)-DF(0) energy transition[14].

Fig. 8 quantitatively shows various maximum small signal gain (SSG) distributions with respect to longitudinal distance from the nozzle exit plane. In general, the maximum SSG is an important key factor in determining the laser beam power for all vibrational transitions, because only one line of largest gain is obtained for each vibrational transition in steady state[15]. As already explained Fig. 7, it is also observed in Fig. 8 that the maximum SSG for the v_{1-0} transition, that is in charge of most of laser power generation, is higher for the case of 388.64 torr than that for the case of 192 torr. For v_{2-1} and v_{3-2} transitions, a very high peak appears for the case of 388.64 torr near the inlet (1~2 *cm*). And for the v_{4-3} transition that almost never affects the production of laser power[14], the maximum SSG for the 192 torr D_2 injection pressure is higher than that for the 388.64 torr over the almost entire range.

The lasing power generated in the resonator is plotted in Fig. 9, which reveals that the highest power is extracted close to the inlet and its maximum peak value (~940 *W/m*) for the case of 388.64 torr is much higher than that (~660 *W/m*) for the case of 192 torr. The total laser beam power of 39.163 *kW/m* is also higher for the case of 388.64 torr than that of 35.853

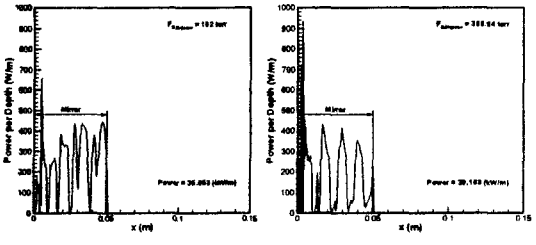

(a) $P_{D2\ Injector}$ = 192 torr (b) $P_{D2\ Injector}$ = 388.64 torr

Fig. 9 Power distributions with respect to longitudinal distance x from the nozzle exit plane

kW/m for the case of 192 torr with the 5 *cm* resonator in this system.

Conclusion

The DF chemical laser involves very complex transport phenomena and chemical reaction to produce the population inversion. In the present study, in order to simulate it, a numerical modeling was introduced considering a consumption of F atom and production of the excited DF molecules. Thereby, the maximum small signal gains could be obtained. Simultaneously, the effects of the D_2 injection pressure on the population inversion with concurrent lasing in the DF chemical laser cavity were discussed. The power generation of the DF chemical laser system could be also determined by the amount of the excited DF molecules produced in the laser cavity. Major results showed that as D_2 injection pressure increases, more F atoms are consumed so that more excited DF molecules in high energy level are produced. In the resonator, a stronger population inversion occurs for all transitions except DF(1)-DF(0) when D_2 injection pressure is lower. However, the high D_2 injection pressure condition makes the difference between DF(1) and DF(0) larger, which is more favorable for generating the higher power. When D_2 injection pressure is higher, the maximum small signal gain in the $v_{1\text{-}0}$ transition, which mainly accounts for generating laser power, becomes higher. Thereby, the total laser beam power extracted also gets higher.

Acknowledgement

The financial assistance by the Combustion Engineering Research Center at KAIST is gratefully acknowledged.

References

1) Emanuel, G.: Analytical Model for a Continuous Chemical Laser, *Journal of Quantitative Spectroscopy and Radiative Transfer*, **11**, 1971, pp.1481-1520.
2) Skifstad, J. G.: Theory of an HF Chemical Laser, *Combustion Science and Technology*, **6**, 1973, pp.287-306.
3) King, W. S., and Mirels, H.: Numerical Study of a Diffusion-Type Chemical Laser, *AIAA Journal*, **10**, 1972, pp.1647-1654.
4) Hofland, R., and Mirels, H.: Flame-Sheet Analysis of C. W. Diffusion-Type Chemical Laser, I. Uncoupled Radiation, *AIAA Journal*, **10**, 1972, pp.420-428.
5) Hofland, R., and Mirels, H.: Flame-Sheet Analysis of C. W. Diffusion-Type Chemical Laser, II. Coupled Radiation, *AIAA Journal*, **10**, 1972, pp.1271-1280.
6) Driscoll, R. J.: Mixing Enhancement in Chemical Lasers, Part I: Experiments, *AIAA Journal*, **24**, 1986, pp.1120-1126.
7) Driscoll, R. J.: Mixing Enhancement in Chemical Lasers, Part II: Theory, *AIAA Journal*, **25**, 1987, pp.965-971.
8) Masuda, W., Satoh, M., Fujii, H., and Atsuta, T.: Numerical Simulation of a Supersonic Flow Chemical Oxygen-Iodine Laser Solving Navier-Stokes Equations, *JSME International Journal Series B*, **40**, 1997, pp.87-92.
9) Gross, R. W. F., and Bott, J. F. *Handbook of chemical lasers*, John Wiley & Sons, New York, 1976.
10) Roe, P. L.: Approximate Riemann Solvers, Parameter Vectors and Difference Schemes, *Journal of Computational Physics*, **43**, 1981, pp.357-372.
11) Yee, H. C.: Construction of Explicit and Implicit Symmetric TVD Schemes and Their Applications, *Journal of Computational Physics*, **68**, 1987, pp.151-179.
12) Yee, H. C.: A Class of High Resolution Explicit and Implicit Shock-Capturing Methods, NASA TM 101099.
13) Jameson, A., and Turkel, E.: Implicit Schemes and LU Decompositions, *Mathematics of Computation*, **37**, 1981, pp.385-397.
14) Spencer, D. J., Mirels, H., and Jacobs, T. A.: Comparison of HF and DF Continuous Chemical Lasers: I. Power, *Applied Physics Letters*, 16, 1970, pp.384-386.
15) Ramshaw, J. D., Mjolsness, R. C., and Farmer, O. A.: Numerical Method for Two-Dimensional Steady-State Chemical Laser Calculations. *Journal of Quantitative Spectroscopy and Radiative Transfer*, **17**, 1977, pp.149-164.

Nomenclature

E, F	inviscid flux vectors
E_v, F_v	viscous flux vectors
I	intensity (W/m^2)
J	*Jacobian*, $\xi_x\eta_y - \eta_x\xi_y$
M	Mach number
n_i	i th species molar concentration (mol/m^3)
N_A	Avogadro number (mol^{-1})
P	mixture pressure (Pa)
Q	conservative state vector

R_u universal gas constant ($J/kmol\ K$)
S source vector
T temperature (K)
t time (s)
x, y Cartesian coordinates (m)
W_i i th species molecular weight ($kg/kmol$)

Greek Symbols

α gain coefficient (cm^{-1})
ξ, η generalized curvilinear coordinates
$\hbar$ Planck's constant ($6.6260755\times10^{-34}\ J\cdot s$)
ν transition frequency (s^{-1})

Superscripts

– non-dimensional quantities

Subscripts

J rotational quantum number
v vibrational quantum number